Dalton Transactions

Radical qubits photo-generated in acene-based metal-organic frameworks

Journal:	*Dalton Transactions*
Manuscript ID	DT-COM-11-2023-003959.R1
Article Type:	Communication
Date Submitted by the Author:	11-Dec-2023
Complete List of Authors:	Orihashi, Kana; Kyushu University, Chemistry and Biochemistry Yamauchi, Akio; Kyushu University, Applied Chemistry Inoue, Miku; Kyushu University, Applied Chemistry Parmar, Bhavesh; Kyushu University, Applied Chemistry Fujiwara, Saiya ; RIKEN Kimizuka, Nobuo; Kyushu University - Ito Campus, Chemistry and Biochemistry Asada, Mizue; Institute for Molecular Science Nakamura, Toshikazu; Institute for Molecular Science Yanai, Nobuhiro; Kyushu University, Applied Chemistry

COMMUNICATION

Radical qubits photo-generated in acene-based metal-organic frameworks

Received 00th January 20xx,
Accepted 00th January 20xx

DOI: 10.1039/x0xx00000x

Kana Orihashi,[‡a] Akio Yamauchi,[‡a] Miku Inoue,[a] Bhavesh Parmar,[a] Saiya Fujiwara,[b] Nobuo Kimizuka,[a] Mizue Asada,[c] Toshikazu Nakamura,[c] and Nobuhiro Yanai*[a,d]

A series of metal-organic frameworks (MOFs) assembled with diazatetracene (DAT)-based linkers are synthesized and characterized. Despite different chromophore orientations and spacings, photoinduced persistent radicals were generated in all the MOFs, and their spin-lattice relaxation time (T_1) and spin-spin relaxation time (T_2) are found to be relatively long even at room temperature. The generality of long T_1 and T_2 of photogenerated radicals in the chromophore-assembled MOFs provides a new platform towards quantum sensing applications.

Electron spins embedded in molecular-based porous materials are promising qubit candidates in quantum information science. The nanoporous structures and the interaction between the host electron spins and the guest molecules offer a promising platform for quantum sensing in the field of chemistry and biology.[1–6] Several kinds of porous systems have been proposed, such as metal-organic frameworks (MOFs) containing paramagnetic metal centre,[1,7–10] MOFs and covalent-organic frameworks (COFs) with organic radicals,[6,11–15] and chromophore triplets in MOFs.[16] A key challenge in applying these materials to quantum science is to extend the coherence time or spin-spin relaxation time (T_2), which is the lifetime of the superposition quantum states. As this superposition state is easily collapsed by interactions with the environment, such as magnetic noise from surrounding nuclear spin motion or paramagnetic species,[17] it is still challenging to realise long T_2 in the MOF especially at room temperature, which is relevant for many bio-sensing applications.

The formation of radicals by photoinduced charge separation has been studied in several MOF systems, mainly for applications as photocatalysts[18] and semiconductors[19]. However, there had been no study aimed at their characterizations as qubits and applications for quantum sensing. We have recently developed a dense chromophore-integrated MOF, which exhibits photoinduced radicals with significantly long spin-lattice relaxation time (T_1) and T_2 values even at room temperature.[6] Our previous MOF system (DAT-MOF-1) consists of the ligand containing 5,12-diazatetracene (DAT) chromophore[20] and the 4,4'-biphenyldicarboxylic acid (BPDC) co-ligand bound to Zn-paddlewheel units. The co-ligand and Zn paddlewheels are considered to be redox inert species.[21] The origin of the radical species was assumed to be charge separation between two DAT chromophores known as symmetry-breaking charge separation (SB-CS).[22–26] The DAT radicals in this MOF exhibited significantly long T_1 and T_2, which were assumed to be partly due to the suppression of DAT mobility by forming π-stacking with the co-ligand BPDC in the interpenetrated MOF structure. However, the necessary conditions for photoinduced radical generation and its long T_1 and T_2 are still unclear and require more systematic investigation.

In this work, we report the synthesis of two new DAT-based MOFs (DAT-MOF-2, DAT-MOF-3) by changing the carboxylate co-ligand and the generality of photoinduced generation of persistent DAT radicals with long T_1 and T_2 values. The use of different co-ligands made it possible to systematically change the structure around the DAT chromophore. Continuous wave-electron spin resonance (CW-ESR) measurements confirmed that the persistent radicals of DAT were generated in the two new MOFs by light irradiation even when different co-ligands were used. Furthermore, pulsed ESR measurements showed that the radicals in the two new MOFs also exhibited shorter T_2

[a] *Department of Applied Chemistry, Graduate School of Engineering*, Center for Molecular Systems (CMS), Kyushu University, 744 Moto-oka, Nishi-ku, Fukuoka 819-0395, Japan. E-mail: yanai@mail.cstm.kyushu-u.ac.jp
[b] RIKEN Center for Emergent Matter Science, Riken, Wako, Saitama 351-0198, Japan
[c] Institute for Molecular Science, Nishigonaka 38, Myodaiji, Okazaki 444-8585, Japan
[d] FOREST, *CREST,* JST, Honcho 4-1-8, Kawaguchi, Saitama 332-0012, Japan.
†Electronic Supplementary Information (ESI) available: See DOI: 10.1039/x0xx00000x
‡ These authors contributed equally to this work.

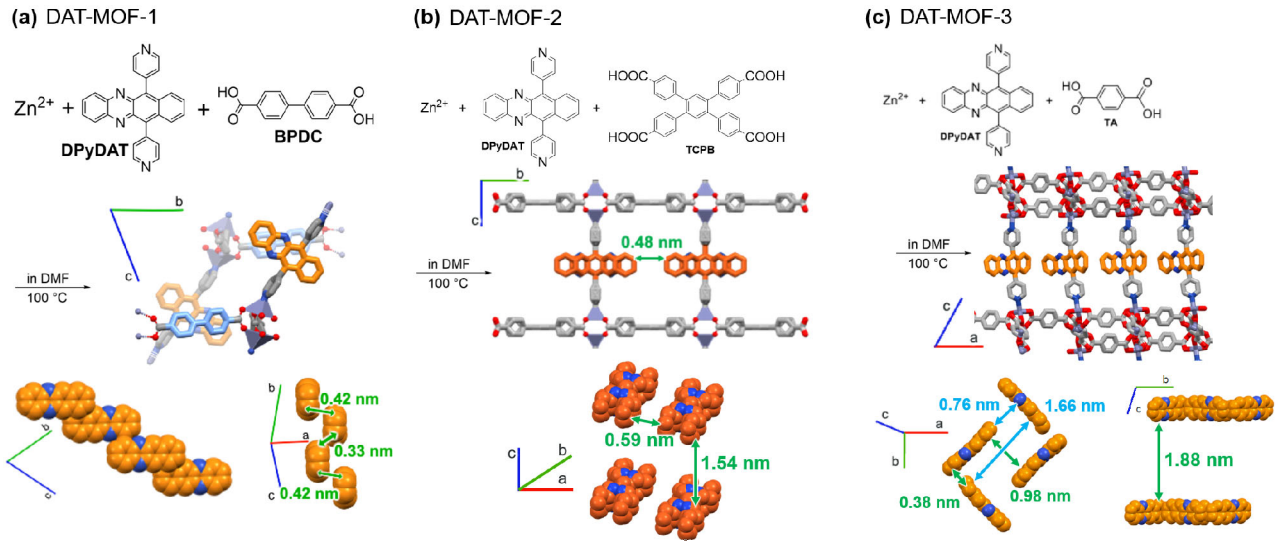

Figure 1 Synthetic scheme, crystal structure and the arrangement of DAT units of (a) DAT-MOF-1, (b) DAT-MOF-2, and (c) DAT-MOF-3.

values than those in the original DAT-MOF-1, implying the critical role of the dynamics of DAT moieties in the MOF structure. The findings on the generality of the photo-generation of persistent radicals in the DAT-based MOFs and the effect of MOF structure on the T_2 of radicals provide important guidance for future quantum sensing using MOFs.

As in the previous report, 6,11-di(pyridine-4yl)benzo[b]phenazine (DPyDAT) modified with pyridine groups as metal coordination sites was used as the DAT-containing ligand. DAT-MOF-1 $[Zn_2(BPDC)_2(DPyDAT)]_n$ was synthesized by solvothermal reaction at 100 °C for 24 h from a DMF solution of $Zn(NO_3)_2{\cdot}6H_2O$, DPyDAT and BPDC in a molar ratio of 2:2:1 according to our previous report. Using different co-ligands, 1,2,4,5-tetrakis(4-carboxyphenyl)benzene (TCPB) and terephthalic acid (TA), DAT-MOF-2 $[Zn_2(TCPB)(DPyDAT)]_n$ and DAT-MOF-3 $[Zn_2(TA)_3(DPyDAT)]_n$ were synthesized under the similar conditions.[27]

Single crystal structure analysis revealed the structural details of the DAT arrangement in each MOFs (Figure 1) ([CCDC 2309918] for DAT-MOF-2 and [CCDC 2309924] for DAT-MOF-3). DAT-MOF-1 and DAT-MOF-2 have two-dimensional sheets of Zn paddle-wheel dimers and co-ligands cross-linked by DPyDAT pillars, resulting in pillared layer-type frameworks. The three-dimensional network of DAT-MOF-1 is doubly interpenetrated, whereas DAT-MOF-2 has a non-interpenetrated single network structure. TCPB has been used to form the non-interpenetrated MOFs with Zn metal ions and bulky pyridyl ligands.[28,29] In the DAT-MOF-1 structure, DAT and BPDC in two different networks form π-π stacking with the carbon-carbon distance of around 0.35 nm, and the DAT unit showed no structural disorder. There is no π-π stacking between the neighbouring DAT units, and the distance between the closest carbon atoms is 0.33nm. In the non-interpenetrated DAT-MOF-2, the DAT unit does not form any π-π stacking, and there is space around the DAT unit, which leads to a disorder in the DAT position. The closest distance between edges of DAT is 0.48 nm, and the core-to core distance between DAT units is 0.59 nm. DAT-MOF-3 also consists of a pillared-layer three-dimensional single network. The bi-layer sheets composed of Zn ions and TA co-ligands are cross-linked by DPyDAT. The DAT units are arranged in a zigzag chain in a double row, and there are no π-π stacking between the neighbouring DAT units. The closest carbon-carbon distance between DAT edges is 0.43nm, and the distance between the double row is 0.60 nm. These results show that DAT forms π stacks with adjacent co-ligands in DAT-MOF-1, while DAT does not form π stacks in DAT-MOF-2 and DAT-MOF-3.

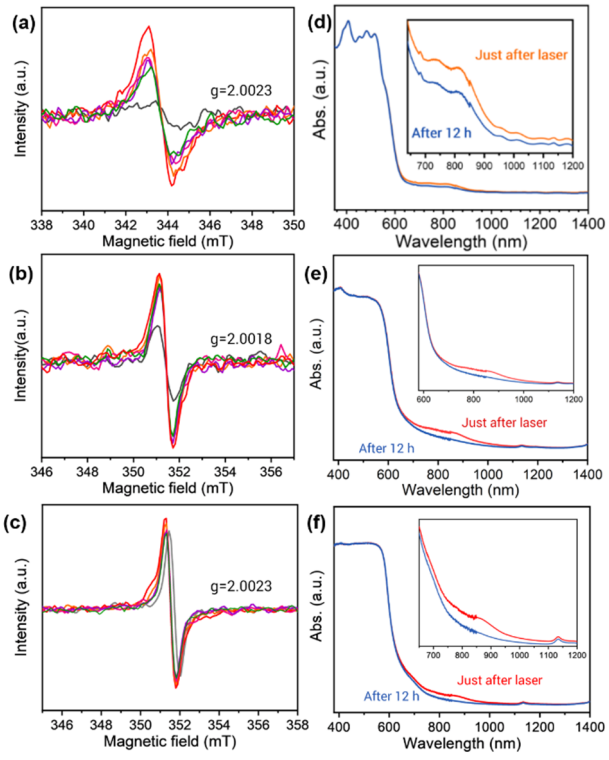

Figure 2. Continuous wave (CW) ESR spectrum of (a) DAT-MOF-1, (b) DAT-MOF-2, and (c) DAT-MOF-3 before laser irradiation (gray lines), immediately after laser irradiation (red lines), and 10 min (orange lines), 30 min (pink lines), 60 min (purple lines), and 90 min (green lines) after laser irradiation. Microwave frequency of each measurement was (a) 9.622124 GHz, (b) 9.842161 GHz, (c) 9.839015 GHz, respectively. UV-Vis absorption spectra of (d) DAT-MOF-1, (e) DAT-MOF-2, and (f) DAT-MOF-3 immediately after (orange, red, and pink line, respectively) and 12 h after light irradiation (blue lines). Pulsed laser

irradiation with wavelength, frequency, power, and duration of 532 nm, 10 Hz, 7.6 mJ, and 20 min were used, respectively.

The purity of the bulk crystals of these three types of MOFs was confirmed by elemental analysis and good agreement of the powder X-ray diffraction (PXRD) patterns with the simulated patterns (Figure S3). The thermo-gravimetric profiles of the three MOFs indicate that the thermal stability of the DAT-MOF series is up to around 300 °C (Figure S4).

The photoinduced persistent radical generation of DAT-MOFs was evaluated by CW-ESR measurements. In our previous report, the typical aromatic radical g value of 2.0023 was observed in DAT-MOF-1.[6,30] The observed radicals were assumed as oxidized/reduced DAT molecules formed by photoinduced charge separation. We observed similar values for DAT-MOF-2 (g = 2.0018) and DAT-MOF-3 (g = 2.0023) (Figure 2a-c). The obtained g values indicate that the similar radical generation by charge separation also occurs in DAT-MOF-2 and 3. To examine the persistence of radical species, CW-ESR measurements were performed before laser irradiation, immediately after laser irradiation, and 10, 30, 60, 90 min after laser irradiation. In all types of MOFs, the signal intensity became stronger by laser irradiation, suggesting the photoinduced radical generation. The fact that the radical signal was observed even in the sample before laser irradiation is probably due to light exposure during the MOF synthesis and sample preparation. Importantly, the intensity of the CW-ESR signal was maintained even 90 min after laser irradiation for all the three MOFs. These results indicate that, despite the different DAT arrangements in each MOF, photoinduced generation of persistent radicals is a general phenomenon.

The formation of radicals of the DAT chromophore in each MOF was further verified by optical spectroscopy. We have confirmed the formation of DPyDAT ligand radicals in DAT-MOF-1 by the difference in absorption spectra between immediately after laser irradiation and 12 h after laser irradiation in our previous report. In addition to the ligand-derived absorption band below 600 nm, a new broad absorption band between 600-900 nm has appeared immediately after laser irradiation, and its intensity decreased after 12 h in the dark.[6,31] Since the new broad absorption band also appeared in the chemically oxidized DAT-MOF-1, the generation of DAT cation radical by photo-irradiation was indicated. Figure 2d-f show the absorption spectra of DAT-MOF-2 and DAT-MOF-3 right after the laser irradiation and 12 h after the laser irradiation. Similar to the case of DAT-MOF-1, both DAT-MOF-2 and DAT-MOF-3 showed characteristic absorption bands between 600-900 nm, and the intensity of this broad band decreases after 12 h. These results suggest that the generation of DAT cation radicals by photo-irradiation also occurs in DAT-MOF-2 and DAT-MOF-3 as in DAT-MOF-1.

The spin-lattice relaxation time (T_1) of the photogenerated radical in each MOF was measured by pulse ESR at room temperature using an inversion recovery sequence (Figure 3a). Measurements were taken at the magnetic field of the radical peak after laser-irradiation. All MOFs showed T_1 values over 100 μs, indicating that the radicals in DAT-based MOF systems generally have a long T_1 at room temperature.

Finally, Hahn-echo sequence (Figure 4b) was used to evaluate the coherence time (T_2) of the radicals in each MOFs at the emission peak of the radicals (343 mT). For all of MOFs, T_2 in the sub-microsecond range were observed at room temperature.

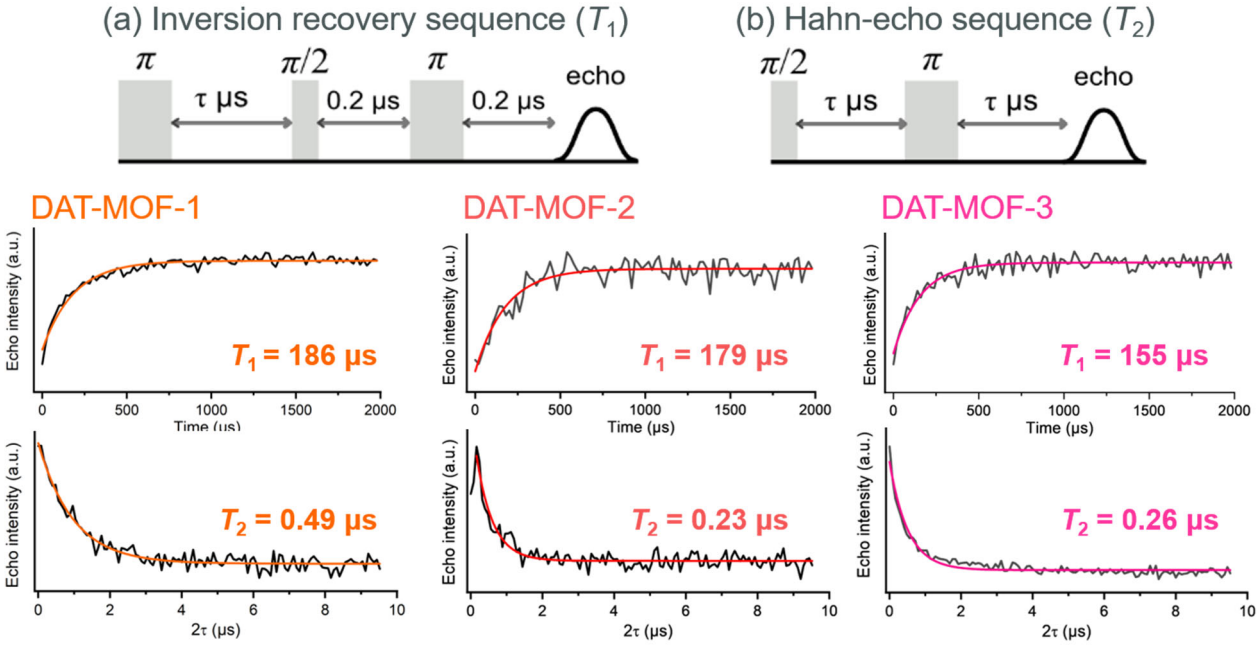

Figure 3 (a)Sequence of inversion recovery and (b) sequence of Hahn-echo sequence of pulsed ESR measurements. Decay of the echo intensity of inversion recovery(top) and Hahn-echo sequence(bottom) of (c)DAT-MOF-1, (d)DAT-MOF-2, (e)DAT-MOF-3, respectively. Single-exponential fitting curve for the decay signal is also shown (orange, red, pink line, respectively). Prior to each measurement, pulsed laser irradiation with wavelength, frequency, power, and duration of 532 nm, 30 Hz, 2 mJ, and 5 min were applied, respectively.

As was the case with T_1, the generality of the long T_2 for the photoinduced persistent radical in the DAT-based MOF system has been confirmed. The relatively long T_2 for all these MOFs suggests that this DAT-based MOF systems could be an excellent candidate for quantum sensing applications. The T_2 value in DAT-MOF-1 is almost double that of the other two MOFs. Focusing on the structure around DAT, the co-ligands are π-stacked on the DAT moieties in DAT-MOF-1, whereas DAT does not form π-stacking in DAT-MOF-2 and DAT-MOF-3. Therefore, the molecular mobility of DAT would be more suppressed in DAT-MOF-1 than in DAT-MOF-2 and DAT-MOF-3, which can be responsible for the T_2 elongation in DAT-MOF-1.

In conclusion, we have successfully observed the formation of photoinduced persistent radicals with relatively long T_1 and T_2 even at room temperature in several MOFs with a high density of DAT chromophores. In addition to the previously reported DAT-MOF-1, two new MOFs were synthesized using the same DAT-containing ligand. Although the arrangements of DAT in each MOF structure are different, the generation of persistent DAT radicals by photocharge separation was observed in all of the three MOFs. Both T_1 and T_2 of the radicals in these MOFs are relatively long at room temperature, indicating that this is a general property of MOFs composed of DAT. The longest T_2 was observed in DAT-MOF-1, suggesting that the suppression of molecular motion by π-stacking is the key to the extended T_2 value. These results suggest a unique material design guideline for the construction of superior qubits in MOFs and are expected to lead to quantum sensing of specific guest molecules by constructing more diverse structures in the future.

Author Contributions

K.O. and N.Y. designed the project. K.O. and A.Y. prepared and characterized materials with a help of M.I., S.F. and N.K. B.P. contributed to the crystal structure analysis. M.S. and T.N. conducted pulse ESR measurements. K.O. and N.Y. wrote the manuscript with contributions from all authors.

Conflicts of interest

There are no conflicts to declare.

Acknowledgements

This work was partly supported by the JST-FOREST Program (JPMJFR201Y), the JST-CREST Program (JPMJCR23I6), JSPS KAKENHI (JP22K19051, JP23H00304, JP21J21996, and JP23KJ1694), Kyushu University Platform of Inter-/Transdisciplinary Energy Research (Q-PIT) through its “Module-Research Program”, Kyushu University Integrated Initiative for Designing Future Society. Part of this work was conducted at Institute for Molecular Science, supported by Advanced Research Infrastructure for Materials and Nanotechnology (JPMXP1222MS0010), and by Nanotechnology Platform Program <Molecule and Material Synthesis> (JPMXP09S21MS0038), of the Ministry of Education, Culture, Sports, Science and Technology (MEXT), Japan.

References

1 A. Kultaeva, A. Pöppl and T. Biktagirov, Atomic-Scale Quantum Sensing of Ensembles of Guest Molecules in a Metal-Organic Framework with Intrinsic Electron Spin Centers, *J. Phys. Chem. Lett.*, 2022, **13**, 6737–6742.

2 M. Atzori and R. Sessoli, The Second Quantum Revolution: Role and Challenges of Molecular Chemistry, *J. Am. Chem. Soc.*, 2019, **141**, 11339–11352.

3 C.-J. Yu, S. von Kugelgen, D. W. Laorenza and D. E. Freedman, A Molecular Approach to Quantum Sensing, *ACS Cent. Sci.*, 2021, **7**, 712–723.

4 M. R. Wasielewski, M. D. E. Forbes, N. L. Frank, K. Kowalski, G. D. Scholes, J. Yuen-Zhou, M. A. Baldo, D. E. Freedman, R. H. Goldsmith, T. Goodson, M. L. Kirk, J. K. McCusker, J. P. Ogilvie, D. A. Shultz, S. Stoll and K. B. Whaley, Exploiting chemistry and molecular systems for quantum information science, *Nature Reviews Chemistry*, 2020, **4**, 490–504.

5 L. Sun, L. Yang, J.-H. Dou, J. Li, G. Skorupskii, M. Mardini, K. O. Tan, T. Chen, C. Sun, J. J. Oppenheim, R. G. Griffin, M. Dincă and T. Rajh, Room-Temperature Quantitative Quantum Sensing of Lithium Ions with a Radical-Embedded Metal-Organic Framework, *J. Am. Chem. Soc.*, 2022, **144**, 19008–19016.

6 K. Orihashi, A. Yamauchi, S. Fujiwara, M. Asada, T. Nakamura, J. K.-H. Hui, N. Kimizuka, K. Tateishi, T. Uesaka and N. Yanai, Spin-Polarized Radicals with Extremely Long Spin-Lattice Relaxation Time at Room Temperature in a Metal-Organic Framework, *ChemRxiv*, , DOI:10.26434/chemrxiv-2023-2mrsw.

7 C.-J. Yu, S. von Kugelgen, M. D. Krzyaniak, W. Ji, W. R. Dichtel, M. R. Wasielewski and D. E. Freedman, Spin and Phonon Design in Modular Arrays of Molecular Qubits, *Chem. Mater.*, 2020, **32**, 10200–10206.

8 J. M. Zadrozny, A. T. Gallagher, T. D. Harris and D. E. Freedman, A Porous Array of Clock Qubits, *J. Am. Chem. Soc.*, 2017, **139**, 7089–7094.

9 C.-J. Yu, M. D. Krzyaniak, M. S. Fataftah, M. R. Wasielewski and D. E. Freedman, A concentrated array of copper porphyrin candidate qubits, *Chem. Sci.*, 2019, **10**, 1702–1708.

10 M. J. Graham, J. M. Zadrozny, M. S. Fataftah and D. E. Freedman, Forging Solid-State Qubit Design Principles in a Molecular Furnace, *Chem. Mater.*, 2017, **29**, 1885–1897.

11 A. K. Oanta, K. A. Collins, A. M. Evans, S. M. Pratik, L. A. Hall, M. J. Strauss, S. R. Marder, D. M. D’Alessandro, T. Rajh, D. E. Freedman, H. Li, J.-L. Brédas, L. Sun and W. R. Dichtel, Electronic Spin Qubit Candidates Arrayed within Layered Two-Dimensional Polymers, *J. Am. Chem. Soc.*, 2023, **145**, 689–696.

12 S. M. Harvey and M. R. Wasielewski, Photogenerated Spin-Correlated Radical Pairs: From Photosynthetic Energy Transduction to Quantum Information Science, *J. Am. Chem. Soc.*, 2021, **143**, 15508–15529.

13 M. Mayländer, S. Chen, E. R. Lorenzo, M. R. Wasielewski and S. Richert, Exploring photogenerated molecular quartet states as spin qubits and qudits, *J. Am. Chem. Soc.*, 2021, **143**, 7050–7058.

14 M. L. Kirk, D. A. Shultz, P. Hewitt, D. E. Stasiw, J. Chen and A. van der Est, Chromophore-radical excited state antiferromagnetic exchange controls the sign of photoinduced ground state spin polarization, *Chem. Sci.*, 2021, **12**, 13704–13710.

15 M. J. Jellen, M. J. Ayodele, A. Cantu, M. D. E. Forbes and M. A. Garcia-Garibay, 2D Arrays of Organic Qubit Candidates

Embedded into a Pillared-Paddlewheel Metal-Organic Framework, *J. Am. Chem. Soc.*, 2020, **142**, 18513–18521.
16 A. Yamauchi, K. Tanaka, M. Fuki, S. Fujiwara, N. Kimizuka, T. Ryu, M. Saigo, K. Onda, Y. Kobori, K. Miyata and N. Yanai, Room-temperature quantum coherence of entangled multiexcitons in a metal-organic framework, *ChemRxiv*, , DOI:10.26434/chemrxiv-2023-nz6rz.
17 S. Takahashi, I. S. Tupitsyn, J. van Tol, C. C. Beedle, D. N. Hendrickson and P. C. E. Stamp, Decoherence in crystals of quantum molecular magnets, *Nature*, 2011, **476**, 76–79.
18 Y. Li, H. Xu, S. Ouyang and J. Ye, Metal-organic frameworks for photocatalysis, *Phys. Chem. Chem. Phys.*, 2016, **18**, 7563–7572.
19 C. G. Silva, A. Corma and H. García, Metal–organic frameworks as semiconductors, *J. Mater. Chem.*, 2010, **20**, 3141–3156.
20 H. Kouno, Y. Kawashima, K. Tateishi, T. Uesaka, N. Kimizuka and N. Yanai, Nonpentacene Polarizing Agents with Improved Air Stability for Triplet Dynamic Nuclear Polarization at Room Temperature, *J. Phys. Chem. Lett.*, 2019, **10**, 2208–2213.
21 I. I. Vrubel, N. Y. Senkevich, E. V. Khramenkova, R. G. Polozkov and I. A. Shelykh, Electronic structure and optical response of Zn-based metal-organic frameworks, *Adv. Theory Simul.*, 2018, **1**, 1800049.
22 J. M. Giaimo, A. V. Gusev and M. R. Wasielewski, Excited-state symmetry breaking in cofacial and linear dimers of a green perylenediimide chlorophyll analogue leading to ultrafast charge separation, *J. Am. Chem. Soc.*, 2002, **124**, 8530–8531.
23 J. Sung, A. Nowak-Król, F. Schlosser, B. Fimmel, W. Kim, D. Kim and F. Würthner, Direct Observation of Excimer-Mediated Intramolecular Electron Transfer in a Cofacially-Stacked Perylene Bisimide Pair, *J. Am. Chem. Soc.*, 2016, **138**, 9029–9032.
24 C. E. Ramirez, S. Chen, N. E. Powers-Riggs, I. Schlesinger, R. M. Young and M. R. Wasielewski, Symmetry-breaking charge separation in the solid state: Tetra(phenoxy)perylenediimide polycrystalline films, *J. Am. Chem. Soc.*, 2020, **142**, 18243–18250.
25 I. Papadopoulos, M. J. Álvaro-Martins, D. Molina, P. M. McCosker, P. A. Keller, T. Clark, Á. Sastre-Santos and D. M. Guldi, Solvent‐dependent singlet fission in diketopyrrolopyrrole dimers: A mediating charge transfer versus a trapping symmetry‐breaking charge separation, *Adv. Energy Mater.*, 2020, **10**, 2001496.
26 J. Tsurumi, H. Matsui, T. Kubo, R. Häusermann, C. Mitsui, T. Okamoto, S. Watanabe and J. Takeya, Coexistence of ultra-long spin relaxation time and coherent charge transport in organic single-crystal semiconductors, *Nat. Phys.*, 2017, **13**, 994–998.
27 W. Danowski, T. van Leeuwen, S. Abdolahzadeh, D. Roke, W. R. Browne, S. J. Wezenberg and B. L. Feringa, Unidirectional rotary motion in a metal-organic framework, *Nat. Nanotechnol.*, 2019, **14**, 488–494.
28 K. L. Mulfort, O. K. Farha, C. L. Stern, A. A. Sarjeant and J. T. Hupp, Post-synthesis alkoxide formation within metal-organic framework materials: a strategy for incorporating highly coordinatively unsaturated metal ions, *J. Am. Chem. Soc.*, 2009, **131**, 3866–3868.
29 W. Bury, D. Fairen-Jimenez, M. B. Lalonde, R. Q. Snurr, O. K. Farha and J. T. Hupp, Control over Catenation in Pillared Paddlewheel Metal–Organic Framework Materials via Solvent-Assisted Linker Exchange, *Chem. Mater.*, 2013, **25**, 739–744.
30 Q. Li, Q. Zhang, W.-J. Wei, A.-N. Wang, J.-X. Hu and G.-M. Wang, Light actuated stable radicals of the 9-anthracene carboxylic acid for designing new photochromic complexes, *Chem. Commun.* , 2021, **57**, 4295–4298.
31 M. Uebe, K. Kawashima, K. Takahashi and A. Ito, Mesityl-Substituted Acene Radical Cations: Decent Stability Comparable to Their Neutral States under Ambient Light and Air, *Chemistry*, 2017, **23**, 278–281.